

Corrosion Performance of Embedded Steel Bar in Cl⁻-contaminated Limestone Calcined Clay Cement (LC3) at initial stage of hydration

Weiwen Li, Zuhua Xu, Xin Wang, Wei Liu, Yaocheng Wang and Xiaobo Ding*

College of Civil and Transportation Engineering, Shenzhen University

ABSTRACT

Limestone Calcined Clay Cement (LC3) presents brilliant properties in binding Cl⁻ so that the embedded steel bars are probably protected in Cl⁻-contaminated condition, which meets the need of sea sand application. However, the corrosion performance of steel bars embedded in LC3 paste with Cl⁻ is unclear, especially in early age hydration. Thus, a series of experiments were carried out to evaluate the corrosion performance of steel bars on initial and hardened stages of hydration, including concentration of OH⁻ and Cl⁻ in real pore solution, open circuit potential (OCP) and chemical elements of steel bars. In terms of early age hydration, the OCP of steel bars and ions concentration in pore solution indicated that both specimens embedded in PC and LC3 pastes were at a highly corrosion state, however, elemental results showed that no obvious corrosion happened at this stage. With respect to hardened age hydration, visual corrosion could be seen on PC-embedded steel bars, with more Fe³⁺ and O²⁻, in comparison with LC3-embedded one, which was related to the much lower absolute OCP and Cl⁻ concentration in pore solution. Overall, LC3 cement demonstrates protective effect on steel bar in special contaminated-Cl⁻ concentration.

1. INTRODUCTION

It has become a well-known issue in coastal regions that steel-reinforced concrete can be contaminated by high concentration of Cl⁻ from sea sand and subsequent pitting corrosion can be caused [1,2]. To deal with the mentioned issue, a novel composite cement with brilliant Cl⁻ binding capacity known as Limestone Calcined Clay Cement (LC3) has been considered to be applied. LC3 cement has been proved to be a promising civil engineering material for resisting Cl⁻ ingress, according to recent studies [3,4]. Based on some durability-related works of authorized research groups, the superior binding capacity against Cl⁻ ingress after long-term hydration has been highlighted. Scrivener et al. [5,6] indicated that the use of calcined clay in PC increased the quantity of gel hydrates and Al-Fe-mono phase during hydration, which was related to Cl⁻ binding. Shi et al. [7] found that high content of calcium from limestone helped promote mono-carbo-aluminate (Mc) conversion to Fs. With respect to the application on corrosion protection, some of the published literatures [8,9] have studied corrosion behavior of steel bars embedded in hardened pastes/mortars/concretes with admixed and penetrated Cl⁻ through electrochemical measurements and they mainly concluded that replacement of cement with metakaolin, functional substance in calcined clay,

effectively reduced the corrosion rate of steel bars and also improved electrical resistivity of hardened concretes after long-term hydration, which was attributed to Cl⁻ binding capacity.

However, the corrosion performance of steel bars embedded by Cl⁻-contaminated LC3 paste is unclear, especially in early age hydration, in which bars are easily to be corroded before the formation of passivate layer and the yield of gel products and Al-Fe-mono phase. Inspired by this need, the study investigated the bound Cl⁻ in paste, electrochemical corrosion and chemical elements of embedded steel bars.

2. Materials and methods

2.1. Raw material and sample preparation

Calcined clay used in this work was provided by Sinoma International Engineering Co. Ltd, with the mineralogy of metakaolin, quartz and muscovite. Clinker was from Wuhan VCEM Technology Development Co. Ltd. Chemical pure limestone and gypsum was produced by Shanghai Macklin Biochemical Technology Co. Ltd. Chemical compositions of the clinker and calcined clay, tested by XRF, are listed in Table 1.

Table 1 Chemical compositions of calcined clay and clinker

Raw material (%)	SiO ₂	Al ₂ O ₃	Fe ₂ O ₃	CaO	MgO	K ₂ O	Na ₂ O	L
Calcined clay	56.79	35.13	2.06	0.16	0.44	3.55	0.08	0.
Clinker	19.96	4.52	3.69	62.79	2.48	0.82	0.31	1.

The mix design is showed in Table 2. The content of mixed Cl⁻ was 0.36% wt. of binders. The fresh pastes were kept in curing chamber with standard temperature (20±1°C) and relative humidity (96±1%) till testing period.

Table 2 Mix design

Notation	Binder proportion (%)				Introduced Cl ⁻ (wt% of binder)	w/b
	C	CC	LS	GP		
LC3-0.36	50.0	31.4	15.6	3.0	0.36	0.45
PC-0.36	97.0	-	-	3.0	0.36	

Note: C, clinker; CC, calcined clay; LS, limestone; GP, gypsum; W, water.

2.2. Testing methods

A typical three-electrode system was applied to consecutively measure the open circuit potential (OCP) within 4h before paste hardening and single tests were carried out after 1/3/7/14 days of curing after demolded, showed on Figure 1.

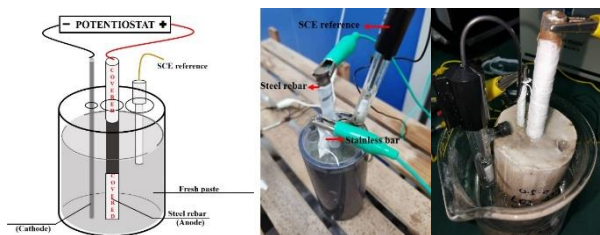


Figure 1. Three-electrode system for electrochemical measurements

The pore solutions of various ages hydration were extracted through compressing machine with controlled stress and corresponding concentration of Cl⁻ and OH⁻ was quantified with titration method and pH probe accordingly. Setup for pore solution extraction is showed on Figure 2. The element of oxygen and ferrum on the embedded steel bars were analyzed by X-ray Photoelectron Spectroscopy (XPS) on an Axis Ultra X-ray photoelectron spectrometer with Al K α excitation.

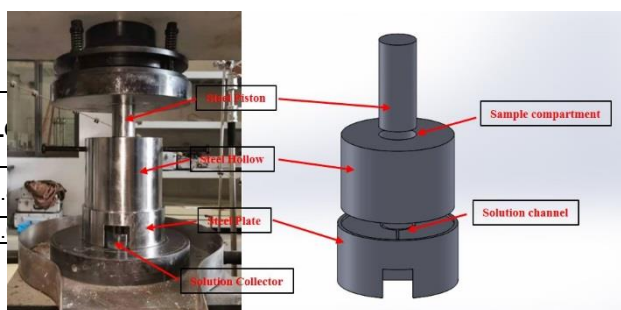


Figure 2. Pore solution extraction equipment

3. Result

3.1 Open circuit potential

To investigate the corrosion activity of reaction on embedded steel bars, the OCP result of PC and LC3 samples is shown in Figure 3. It could be clearly observed on Figure 3, within the 4 hours hydration before hardening, that the OCP of both specimens demonstrated drops at the beginning but gradually got increased after 1.5~2.0 hours of hydration, probably owing to the protection effect of initial and metastable passivity in high alkalinity of fresh paste [10]; it can be also seen that the difference of OCP between inserted bars in LC3 and PC paste, less than around 5%, is quite marginal. It is probably because the formation of C-(A, S)-H and Al-Fe-mono phase in LC3 paste, responsible to Cl⁻ binding, was metastable, which could not bond Cl⁻ effectively enough. With respect to the hardened age hydration, as showed on Figure 3, it could be noticed that with the prolong of hydration period, both samples demonstrated increasing OCP and reached to their peaks within 72~168 hours. Moreover, it could also be found quantitatively that LC3 paste helped increase the maximum value of OCP by 8.5%, compared with PC.

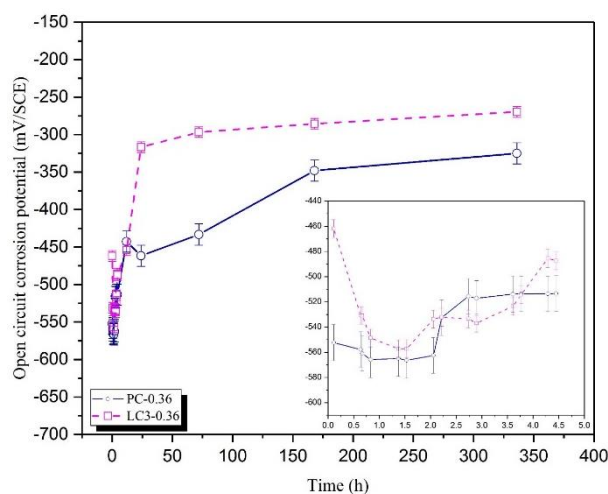


Figure 3. Early stage OCP results for the embedded steel bars in PC and LC3 samples, 4h and 336h

3.2 OH⁻ and Cl⁻ concentration of pore solution

3.2.1 OH⁻ concentration

The concentration of OH^- in pore solution is demonstrated in Figure 4. In the early period of hydration, within 24 hours, the OH^- concentration in PC paste pore solution shown a gradual increasing trend whilst in LC3 pore solution it had an evident drop after 12 hours hydration, owing to consumption of alkaline substance in secondary hydration of pozzolanic calcined clay. From general view of OH^- concentration during early and hardened period of hydration, it could be observed that the OH^- concentration of LC3 pore solution maintained at a relatively low level and reached to a dynamic balance after hydration of 168 hours (7 days), opposite to condition of PC pore solution which had a gradual increase during the whole tested period.

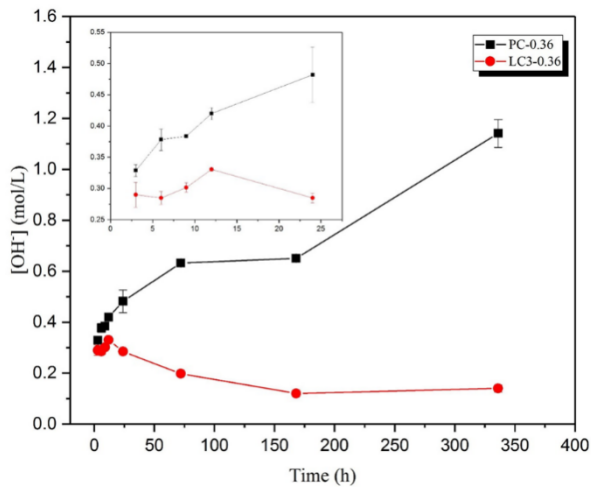


Figure 4. OH^- concentration of pore solution in PC and LC3 hardened paste during 24h and 336h

3.2.2 Cl^- concentration

Figure 5 presents time-dependent Cl^- concentration of pore solution during a period of 24 and 336 hours. On the one hand, during 24 hours of hydration, Cl^- concentration of pore solution in both pastes shown a mild fluctuation within first 12 hours but displayed a sudden drop within the following half, suggesting that large amount of Cl^- began to be bonded during 12 to 24 hours hydration, which is recognized as an important period of Cl^- binding of both PC and LC3 cement. At this stage, it could also be seen that Cl^- concentration in pore solution of LC3 is still higher than that in PC. The main reason for this phenomenon is probably because the calcined clay in LC3 cement initially started to perform their chemical activity and bind Cl^- on the 1st day of hydration, however it might not compensate with the Cl^- binding attributed to another 50% of clinker. On the other hand, for hardened period of hydration, consecutively dramatical decrease could be observed in both solution after 24 hours and it remained a relatively static level after at the age of 7 days, which is thought of as another essential period of Cl^- binding. At this stage, it should be noted that Cl^- concentration of the

pore solution had a sharp drop after 24 hours hydration and thus it showed a lower concentration than that in PC paste.

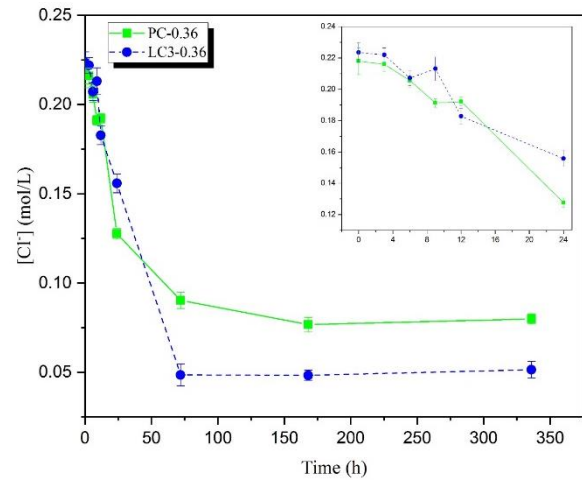


Figure 5. Cl^- concentration of pore solution in PC and LC3 hardened paste during 24h and 336h

3.2.3 Cl^- to OH^- concentration ratio

Based on the mainstream view, the ratio Cl^-/OH^- of pore solution plays a crucial role on steel bar corrosion, because both OH^- and Cl^- are related to the stability of passive film on the rebars [11]. Figure 6 demonstrates the Cl^-/OH^- of real pore solution of PC and LC3 pastes at various ages, showing that the value of both specimens decreased gradually. It was because the decrease of Cl^- was much evident than the increase of OH^- . It should be mentioned that a stable growth of the figure for LC3 pastes can be observed after 72 h, which was mainly because the concentration of OH^- decreased but Cl^- was retained. In addition, it can also be found that the value of LC3 was higher than that of PC, which was a bit different from the prediction. In terms of its explanation, it was probably because the application of the value was mainly based on Portland cement concrete, it is still unclear whether it can be applied to LC3 cement. From another view, contamination of Cl^- was considered as high risk of corrosion, even in case of high alkaline surroundings [2]. Based on this theory, it can be explained that the more corrosive state of embedded bar in PC was related more on higher Cl^- in its pore solution, even though the alkalinity was also higher than that of LC3.

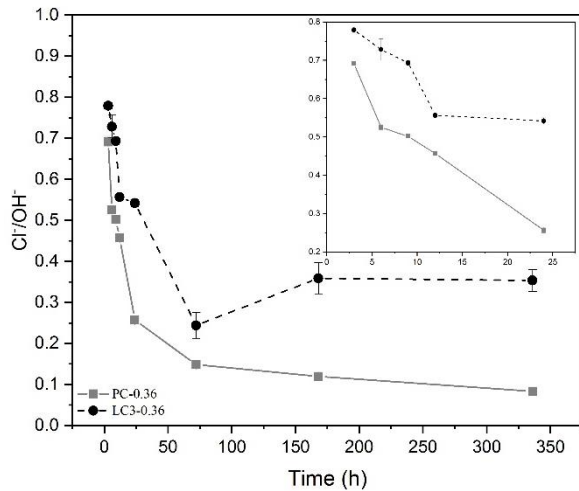


Figure 6. Concentration Cl^-/OH^- of pore solution at during 24h and 336h

3.3 Chemical elements of ferrum and oxygen

Figure 7 demonstrates the surficial condition of exposed areas of steel bars, with a clarity for testing area of XPS spectra. As can be seen, after 12 hours of corrosion, there was no visual rust on both PC and LC3-embedded steel bars. However, with the age extended until 336 hours, visual corrosion was observed on PC-embedded bar, whilst there was still no obvious rust on the LC3-embedded one.

The surficial elements of inserted rebars at hydration age of 12 and 336 hours were studied by XPS in Figure 8. In the high-resolution spectra of Fe 2p and O 1s, all specimens demonstrate similar curve shape, where four typical peaks of Fe 2p and two peaks of O1s are identified based on some of the authorized studies [12,13]. Precisely, three typical peaks locate at approximately 710.9eV, 713.0eV and 725.5eV, corresponding to Fe $2p_{3/2}$ and Fe $2p_{1/2}$, with a satellite peak in the middle, which refer to the binding energy of Fe^{3+} in Fe_2O_3 . Regarding oxygen, showed on Figure 8 (b), it can be observed the curve can be separated from two typical peaks, locating at around 529.8eV and 531.6eV accordingly and corresponding to chemisorbed oxygen (O_c , associated to bound hydroxyl groups) and lattice oxygen (O_l , associated to O^{2-} in Fe_2O_3).

Compared with the rebars embedded by LC3 and PC pastes, it can be seen that after 12 hours of hydration, the relatively stabilized peaks of Fe and O suggested there were no enormous corrosion products on the surface, indicating that the corrosion was mild. Such phenomenon claimed that in the tested Cl^- concentration, both specimens did not get corroded obviously during a short term, even though the OCP was high. However, with prolong of the age till 336 hours, evident difference happened to the specimens. In comparison, rebar in PC demonstrated much higher and sharper peak than that in LC3, suggesting that LC3 cement presented an effective protection on

the rebars in case of Cl^- contamination, which should be related to its brilliant Cl^- binding effect.



Figure 7. Photographs of embedded steel bars in PC and LC3 pastes for various ages of hydration (shade area refers to XPS specimens)

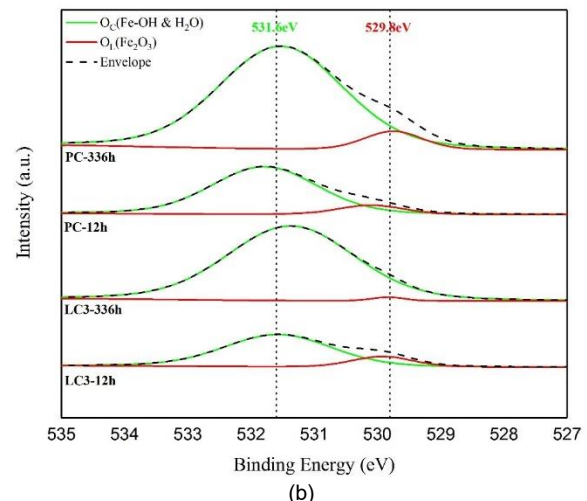
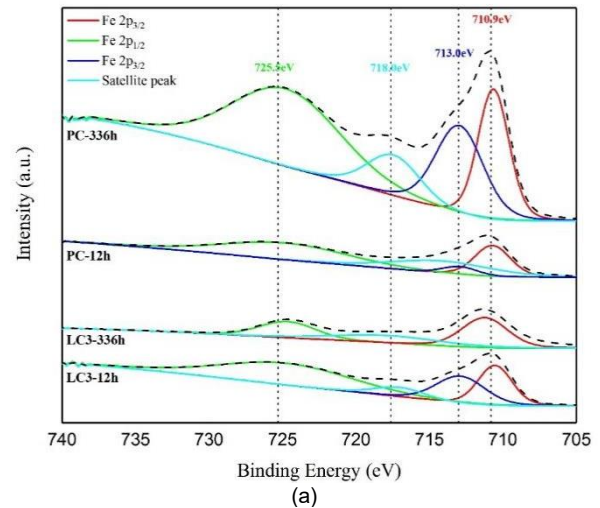


Figure 8. XPS spectra of Fe 2p (a) and O1s (b) of steel bars in PC and LC3 pastes during 12 and 336 hours

4. Conclusion

- During the 1st day of hydration, based on the results of OH^- and Cl^- concentration in squeezed pore solution as well as the OCP, the tested steel bars in either PC or LC3 pastes were corrosively-active, indicating that they were at easily-corroded state. However, the XPS spectra showed there was no visual rust on the surfaces of rebars. It can be concluded that the steel bars

in both pastes were in danger, but no actual damages happen.

- In between the 1st and 14th day, much more obvious rusts were discovered on PC-embedded sample than that embedded by LC3 pastes. The latter demonstrated far lower absolute value of OCP as well as less apparent Fe³⁺ and O²⁻ peaks on XPS spectra.
- Overall, in certain occasion of Cl⁻ contamination, LC3 cement can surely provide effective protection on the embedded steel bars.

Acknowledgments

The authors show strong appreciation towards the financial support provided by the National Natural Science Foundation of China (NSFC Grant Numbers 51878415, 52078301, 51520105012 and 51978408); Natural Science Foundation of Guangdong Province (grant number 2019A1515012014); and the platform built up by Guangdong Provincial Key Laboratory of Durability for Marine Civil Engineering, SZU (grant number 2020B1212060074).

REFERENCES

1. J. Xiao, C. Qiang, A. Nanni and K. Zhang, Use of sea-sand and seawater in concrete construction: Current status and future opportunities. *Construction and Building Materials*, 2017. 155: 1101-1111.
2. W. K. Green, Steel reinforcement corrosion in concrete – an overview of some fundamentals. *Corrosion Engineering, Science and Technology*, 2020. 55(4): 289-302.
3. Y. Dhandapani, T. Sakthivel, M. Santhanam, R. Gettu and R. G. Pillai, Mechanical properties and durability performance of concretes with Limestone Calcined Clay Cement (LC3). *Cement and Concrete Research*, 2018. 107: 136-151.
4. H. Maraghechi, F. Avet, H. Wong, H. Kamyab and K. Scrivener, Performance of Limestone Calcined Clay Cement (LC3) with various kaolinite contents with respect to chloride transport. *Materials and Structures*, 2018. 51(5).
5. K. Scrivener, F. Martirena, S. Bishnoi and S. Maity, Calcined clay limestone cements (LC3). *Cement and Concrete Research*, 2018. 114: 49-56.
6. F. A. Karen Scrivener, Hamed Maraghechi Impacting factors and properties of limestonecalcined clay cements (LC3). *Green Materials*, 2019. 7(1): 3-14.
7. Z. Shi, M. R. Geiker, K. De Weerd, T. A. Østnor, B. Lothenbach, F. Winnefeld and J. Skibsted, Role of calcium on chloride binding in hydrated Portland cement–metakaolin–limestone blends. *Cement and Concrete Research*, 2017. 95: 205-216.
8. Q. D. Nguyen and A. Castel, Reinforcement corrosion in limestone flash calcined clay cement-based concrete. *Cement and Concrete Research*, 2020. 132: 106051.
9. E. Güneysi, M. Gesoğlu, F. Karaboğa and K. Mermerdaş, Corrosion behavior of reinforcing steel embedded in chloride contaminated concretes with and without metakaolin. *Composites Part B: Engineering*, 2013. 45(1): 1288-1295.
10. W. Liu, Y.Q. Li, L.P. Tang and Z.J. Dong, XRD and ²⁹Si MAS NMR study on carbonated cement paste under accelerated carbonation using different concentration of CO₂. *Materials Today Communications*, 2019. 19: 464-470.
11. J. Rao and T. Pan, Efficacy and efficiency of dual electrochemical strategies for remedying rebar corrosion in heterogeneous concrete. *Cement and Concrete Composites*, 2020. 108: 103531.
12. F. Lewis, M. Cloutier, P. Chevallier, S. Turgeon, J.-J. Pireaux, M. Tatoulian and D. Mantovani, Influence of the 316 L Stainless Steel Interface on the Stability and Barrier Properties of Plasma Fluorocarbon Films. *ACS Appl Mater Interfaces*, 2011. 3(7): 2323-2331.
13. D. X. Bo Lei, Bo Wei, Tengfeng Xie, Chunyu Xiao, Weiliang Jin, Lingling Xu, In Situ Synthesis of alpha-Fe₂O₃/Fe₃O₄ Heterojunction Photoanode via Fast Flame Annealing for Enhanced Charge Separation and Water Oxidation. *ACS Appl Mater Interfaces*, 2021. 13(3): 4785-4795.